Femtosecond Transient Absorption, Raman, and Electrochemistry Studies of Tetrasulfonated Copper Phthalocyanine in Water Solutions

H. Abramczyk,*,† B. Brożek-Płuska,*,† K. Kurczewski,*,† M. Kurczewska,*,† I. Szymczyk,*,† P. Krzyczmonik,‡ T. Błaszczyk,‡ H. Scholl,‡ and W. Czajkowski§

Institute of Applied Radiation Chemistry, The Faculty of Chemistry, Technical University of Łódź, Wroblewskiego 15, 93-590 Łódź, Poland, Department of General and Inorganic Chemistry, University of Łódź, Narutowicza 68, 90-136 Łódź, Poland, and Institute of Polymers and Dyes Technology, The Faculty of Chemistry, Technical University of Łódź, 90-924 Łódź, Żeromskiego 116, Poland

Received: January 17, 2006; In Final Form: May 17, 2006

Ultrafast time-resolved electronic spectra of the primary events induced in the copper tetrasulfonated phthalocyanine $Cu(tsPc)^{4-}$) in aqueous solution has been measured by femtosecond pump−probe transient absorption spectroscopy. The primary events initiated by the absorption of a photon occurring within the femtosecond time scale are discussed on the basis of the electron transfer mechanism between the adjacent phthalocyanine rings proposed recently in our laboratory. The femtosecond transient absorption results are compared with the low temperature emission spectra obtained with Raman spectroscopy and the voltammetric curves.

1. Introduction

Photochemistry of phthalocyanines has been studied extensively by various spectroscopic methods for many decades.[1−29] However, femtosecond spectroscopy creates a new quality in photochemical and photophysical research because we can observe the primary events initiated by the absorption of photon.[30−34]

Phthalocyanines belong to a broad group of chemicals, which are potential photosensitizers of the third generation in the photodynamic therapy. Understanding the primary photochemical events is a key step in understanding photobiology and the mechanisms of selective interaction between the photosensitizers and human tissues. It will help to establish mechanisms of energy dissipation, particularly the contribution from the I and II type of oxidation. This knowledge is crucial in efficiency of the photodynamic therapy, because the quantum yields for the reaction of oxidation via generation of radicals or energy transfer between the photosensitizers and the triplet oxygen of the ground state determine the photodynamic activity.

Another important application of phthalocyanines are molecular conductance junctions[35] in which a molecule or a small cluster of molecules conduct electrical current between two electrodes. Copper phthalocyanine (CuPc) has been used in silicon-based molecular nanotechnology[36] as a molecule to integrate molecular electronic function with silicon surfaces. In these applications the knowledge about mechanisms of charge transfer and the role of the outer benzene ring is important to understand the interaction with the surrounding substrate when the CuPs molecule is bound to the surface via its central copper atom.

A first aim of the paper is to provide an experimental and theoretical basis for elucidation of ultrafast electronic dynamics and photochemistry of the early intermediates in phthalocyanine derivatives in aqueous solutions by femtosecond transient absorption and Raman spectroscopy.

A second aim is establishing a close relation between recently calculated properties of the electronic structure of copper phthalocyanines[25] and the experimental optical transitions obtained in this paper. We will show that combining the femtosecond transient absorption spectroscopy, Raman spectroscopy and electrochemical measurements provides a significantly clearer interpretation of the primary events upon light excitation, photochemical mechanisms and spectral features related the these photophysical and photochemical mechanisms.

2. Experimental Section

Copper(II) phthalocyanine-3,4′,4″,4‴-tetrasulfonic acid, tetrasodium salt, was purchased from Aldrich. It was used without further purification. Water was distilled before preparing the solutions.

Zinc phthalocyanine tetrasulfonic acid, tetrasodium salt was prepared by a process similar to that described by Griffiths and co-workers.[37] Thus the mixture of the previously prepared (by the oxidation of 2-hydroxynaphthalene-6-sulfonic acid with potassium manganate)[38] 4-sulfophthalic anhydride (5 g), urea (4 g), ammonium chloride (0.34 g), ammonium molybdate (0.06 g), boric acid (0.06 g), zinc(II) acetate dihydrate (1.1 g) in 10 cm^3 of sulfolane was slowly heated to 90 °C, kept for 1 h and, after addition of further 1 g of urea, heated to 200−210 °C and kept for 1−2 h. After cooling, the reaction mixture was diluted with 20 cm^3 of methanol, filtered and washed on the filter with another 10 cm^3 of methanol. The solid residue was then dissolved in 30 cm^3 of water with the addition of 10% NaOH solution to pH = 8.5 and filtrated after addition of activated carbon. After the solution was evaporated to dryness, 5.4 g of crude dye was obtained. It was purified by twice dissolving in distilled water and precipitation by methanol and finally by the column chromatography first on silica gel and after that on cellulose powder.

The Raman spectra were recorded in the cryostat (Oxford Instruments Limited) with commercial glass ampules that were

† Institute of Applied Radiation Chemistry, The Faculty of Chemistry, Technical University of Łódź. Phone: (+ 48 42) 631-31-88, 631-31-05.
‡ Department of General and Inorganic Chemistry, University of Łódź. Phone: (+ 48 42) 635-58-04.
§ Institute of Polymers and Dyes Technology, The Faculty of Chemistry, Technical University of Łódź. Phone: (+ 48 42) 631-32-31, 636-25-96.

10.1021/jp060322a CCC: $33.50
Published on Web 06/22/2006

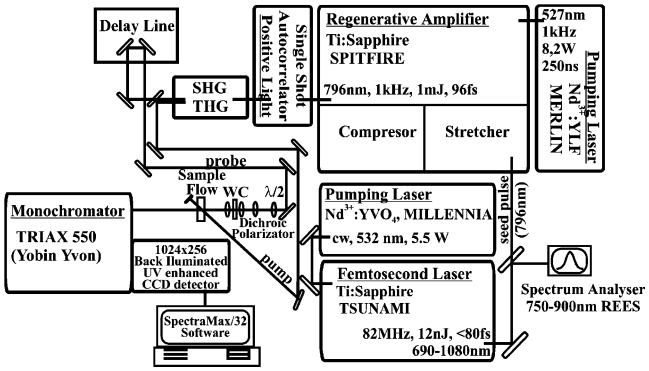

Figure 1. Femtosecond pump−probe experimental setup.

mounted in a special cell arrangement. The samples were introduced as a liquid, and they were cooled in the cryostat equipped with a heater and thermocouples for temperature monitoring. Cooling of the sample was achieved by the use of a 50 L Dewar that supplied a small stream of liquid nitrogen or helium through a vacuum jacketed tube to the cryostat coat. To ensure that the equilibrium phases (crystal polymorphs) are generated, the samples were cooled slowly (0.5 °C/min). The nonequilibrium phases (glasses) were generated at the rapid temperature quenching in a special homemade ring immersed in liquid nitrogen with liquid solutions of $Cu(tsPc)^{4-}$ injected into the ring. This procedure ensures the maximum possible quenching rate, in contrast to the slow cooling of 0.5 °C/min used for generation of the equilibrium phases. The procedure corresponds to the deposition of an amorphous film or direct sublimation of the sample on the cold support at 77 K used previously to obtain phases strongly deviated from equilibrium.[39]

Some samples were deareated by using homemade vacuum line. Each sample containing 1.5 cm^3 of solution was frozen by immersion into liquid nitrogen and after 10 min gases above the sample were drawn out by connecting the sample to a vacuum pump. After the gases were removed, the connection was closed and samples were unfrozen. This procedure was repeated at least five times until the pressure above the frozen sample and the minimum pressure made by the applied vacuum pump were the same and equal to 0.002 mmHg.

Raman spectra were measured with Ramanor U1000 (Jobin Yvon) and Spectra Physics 2017-04S argon ion laser operating at 514 nm at powers of 26 mW, respectively. Raman spectra in the phonon region of 15−200 cm^{-1} and in the region of internal vibrations 200−6000 cm^{-1} (or 200−8000 cm^{-1}) were recorded. The spectra were recorded in a broad temperature range from 293 to 77 K. The spectral slit width was fixed as 6 cm^{-1} in the full temperature range, which corresponds to the 500 μm mechanical slit of the spectrometer. The interference filter has been used to purify the laser line by removing additional natural emission lines that interfere with the Raman lines, especially in the case of the solid samples.

The femtosecond pump−probe experiment has been performed with a setup presented in Figure 1. The laser system is based on the mode-locked titanium sapphire femtosecond laser (Tsunami, Spectra Physics, 796 nm, 82 MHz, 12 nJ, <80 fs), pumped with the second harmonic of the solid state laser Nd^{3+}:YVO_4 (532 nm, continuous wave (cw), Millennia, Spectra Physics). A part of the output of the femtosecond laser is sent to the spectrum analyzer (Rees) to control the quality of the mode-locking. The seed femtosecond pulse is stretched, amplified in the regenerative amplifier and compressed (Spitfire, Spectra Physics, 1 kHz, 1 mJ, 796 nm, 96 fs). The pulse duration is measured with the single shot autocorrelator (Positive Light). The regenerative amplifier is pumped with the second harmonic (Nd:YLF, 527 nm, Q-switching laser, 250 ns, 1 kHz). The second harmonic (398 nm) is generated on KD*P crystal in the I type phase matching process and is used as a pump pulse of energy 0.03 mJ. The fundamental (796 nm) is focused onto the cell of 0.7 mm length with deuterated water to generate white continuum (WC) in the broad range of 300−1000 nm that is used as a probe pulse. The broadband filter (785−850 nm) was placed after WC to suppress the fundamental at 796 nm. The fundamental beam was delayed by a scanning translation stage under computer control, providing path difference increment equivalent to 16 fs. The pump and probe beams with 3 μJ/pulse at 1 kHz repetition rate were focused and overlapped onto a quartz sample cell (0.2 mm, quartz suprasil, transmittance 200−2500 nm, QS, Hellma) containing $Cu(tsPc)^{4-}$ in water. The sample was continually refreshed by flowing the sample with a peristaltic pump. Attention was paid to adjust the circulation speed in the order the sample was replaced after each laser shot.

After passing the sample, the light was focused on the entrance slit and dispersed by a $f = 0.75$ m spectrometer (Triax 550, Jobin Yvon) equipped with a 1200 lines/mm grating blazed at 750 nm and detected with a liquid nitrogen cooled CCD camera (1024 × 256, back illuminated, UV enhanced, Jobin Yvon-Spex). The signals from 5 accumulations each with the integration time of 0.02 s were averaged, which corresponds to 100 pulses for each wavelength.

The zero delay was found by detecting the fluorescence of POPOP dye (1,4-bis(5-phenyl-2-oxazolyl)benzene) in DMSO solution caused by a consecutive (1+1′) two-photon excitation. The POPOP absorption maximum is observed at 350 nm, and the fluorescence maximum is at 427 nm. In our experimental setup the dye molecule absorbs photons from the 796 nm (two-photon absorption) and a photon from 398 nm pulse laying in the lower frequency wing of the absorption band. The method yields an intensity cross-correlation function for the overlap of the pump and the probe laser beams.

Electrochemical experiments by means of cyclic voltammetry were done using a Par 273A potentiostat operated by an IBM PC computer with CorrWare v.2.8 software. The measurements were carried out in a three-electrode cell. The cell was adapted for simultaneous electrochemical experiments and measurements by means of Raman spectroscopy. The working electrode was a flat gold electrode of geometrical area 0.196 cm^2. The construction of the cell enabled a free rotation of the working electrode of 360°. In this way it was possible to position the surface of the electrode suitable of the incident light. The counter electrode was sheet platinum and a saturated in NaCl calomel electrode (saturated in NaCl) was used as the reference electrode. The reference electrode was connected with the examined solution by means of electrolytic bridge with Lugin's capillary. Voltammetric measurements of phthalocyanine of copper were done in aqueous solutions of concentrations 10^{-3} and 10^{-5} mol/dm^3. Before the measurements the solutions were deaerated by means of argon.

3. Results and Discussion

Figure 3a−c shows the temperature dependence of the emission spectra of the sulfonated copper phthalocyanine ($Cu(tsPc)^{4-}$) (Figure 2) obtained by Raman spectroscopy. One can see two characteristic emission bands: with maxima at around 520 nm and at 682 nm and the narrow Raman peaks corresponding to the vibrations of $Cu(tsPc)^{4-}$ and water. The stretching symmetric and asymmetric vibrational bands of water are observed at around 3091 cm^{-1} (at 77 K) and 3270 and 3416

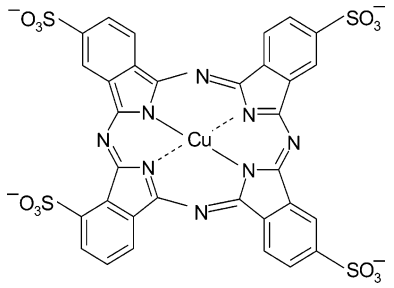

Figure 2. Structure of metal phthalocyanines, copper(II) phthalocyanine-3,4′,4″,4‴-tetrasulfonic anion.

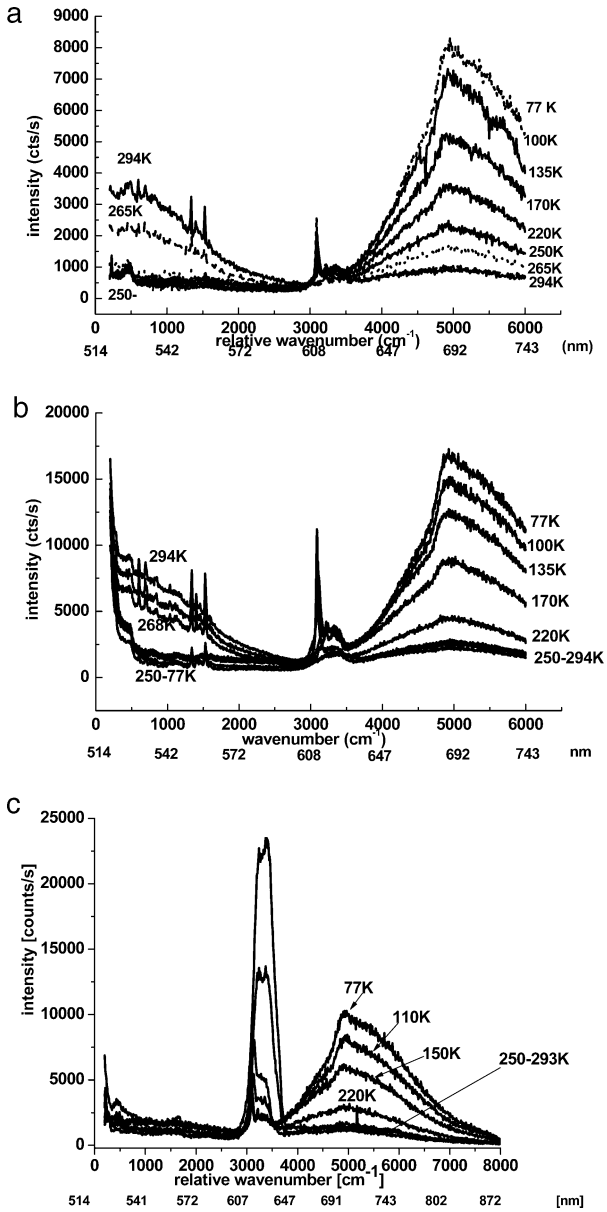

Figure 3. Raman and emission spectra of $Cu(tsPc)^{4-}$ in aqueous solution as a function of temperature at slow cooling rate (0.5 K/min): (a) $c = 0.001$ mol/dm^3, the sample is degassed; (b) $c = 0.001$ mol/dm^3, the sample is nondeaerated; (c) $c = 10^{-5}$ mol/dm^3, the sample is nondeaerated.

cm^{-1} at 294 K (Figure 3b,c). One can see that the intensity of the vibrational band of water strongly depends on the $Cu(tsPc)^{4-}$ concentration. One can see that at higher concentrations of $Cu(tsPc)^{4-}$ ($c = 10^{-3}$mol/dm^3) the band of liquid water disappears (Figure 3a). This effect is due to absorption of phthalocyanine. The copper phthalocyanine has a strong absorption between 550 and 750 nm (Q-band) that partially overlaps with the region of the Raman scattering for the symmetric and asymmetric modes of water. Raman scattering of water is absorbed by the $Cu(tsPc)^{4-}$ molecules and the Raman intensities of the stretching bands of water decrease. At lower concentrations of phthalocyanine where the absorption of $Cu(tsPc)^{4-}$ becomes weaker, Raman scattering from water can be observed and the broad intense band between 3000 and 4000 cm^{-1} (608−647 nm) can be seen in Figure 3b,c. The results in Figure 3a are obtained for degassed samples. Identical spectral features are observed for nondeaerated samples (Figure 3b).

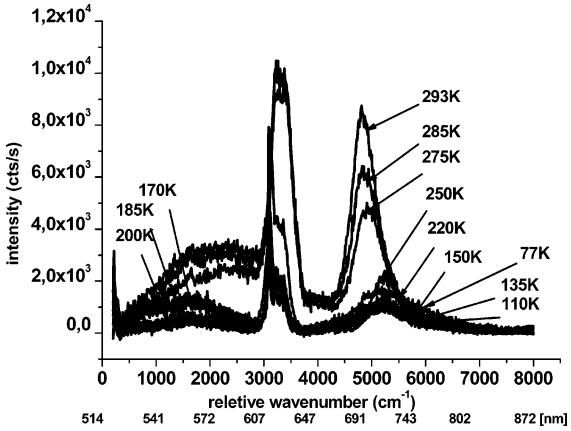

Figure 4. Raman and emission spectra of $Zn(tsPc)^{4-}$ in aqueous solution as a function of temperature at slow cooling rate (0.5 K/min) for $c = 10^{-5}$ mol/dm^3, the sample is degassed.

In this paper we will concentrate on the origin of the emission bands at 520 nm and at 682 nm. Although studied extensively for a few decades, the photochemistry of metal phthalocyanines is still unclear. Most papers[5] have concentrated on the absorption features of the two major bands, namely the B (or Soret) band ($S_0(a_{2u}) \rightarrow S_1(2e_g)$ and $S_0(b_{2u}) \rightarrow S_1(2e_g)$) and the Q-band ($S_0(a_{1u}) \rightarrow S_1(2e_g)$). Both bands have the $\pi \rightarrow p^*$ character with the 2p states of the phthalocyanine rings involved in the transition. The emission spectra of metal phthalocyanines are much less clear although their origins play a crucial role in the photodynamic diagnostic. Especially, the emission at around 500 nm (520 nm for $Cu(tsPc)^{4-}$ in water) has been attributed in the literature to the transitions of very different origins: reduced form $(MePc)^{\bullet -}$[24], $S_2 \rightarrow S_0$ emission for Q-band,[20] $T_n \rightarrow T_1$ emission,[14,40] charge transfer (CT) between the central metal (3d states) and the ligand phthalocyanine states,[40−42] $\pi^* \rightarrow$ n emission,[24] $S_1 \rightarrow S_0$ emission for the B band.[21−22]

The emission in the range 600−700 nm has been interpreted almost exclusively as the emission of the Q-band. However, we have shown recently[1] that the same region is occupied by the emission of some transient species that has been assigned to the transient radicals generated as a result of the electron transfer between the adjacent rings of the stacked structures. These transient products can easily be seen at low temperatures.

Indeed, the results in Figure 3a,b show that the tetrasulfonated copper phthalocyanine ($Cu(tsPc)^{4-}$) has negligible emission between 600 and 740 nm at room temperature or 294 K despite the absorption Q-band at 620 nm (dimer) and 661 nm (monomer).[1] However, at lower temperatures the emission begins to increase significantly with decreasing temperature. The emission due to the fluorescence is expected to decrease rather than increase with decreasing temperature, like for the results presented in Figure 4. Figure 4 shows the photochemical behavior for the tetrasulfonated zinc phthalocyanine ($Zn(tsPc)^{4-}$) in aqueous solution as a function of temperature, and we can

SCHEME 1: Electronic Energy Levels of Copper Phthalocyanine (CuPc) and Zinc Phthalocyanine (ZnPc)[25]

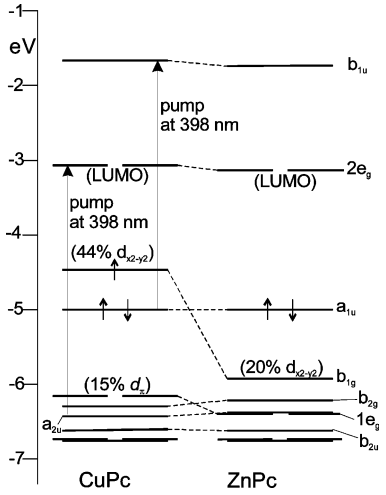

see drastically different behaviors when compared with results in Figure 3a,b. In Figure 4 one can see the emission band with maximum at around 692 nm with the intensity decreasing with decreasing temperature. This type of behavior has been assigned to the "normal" fluorescence of the Q transition. It is simply due to the fact that decreasing the temperature increases the dimerization (or aggregation) with the last species being less fluorescent or nonfluorescent. Comparing Figure 3c and 4 for the same concentration of $Cu(tsPc)^{4-}$ and $Zn(tsPc)^{4-}$, we can see that in contrast to the emission of $Zn(tsPc)^{4-}$ for the liquid and undercooled states (293−275 K in Figure 4) in the range 647−743 nm that decreases with decreasing temperature, the emission of $Cu(tsPc)^{4-}$ is negligible in the liquid phases and begins to increase with decreasing temperature. Moreover, the emission of $Zn(tsPc)^{4-}$ in the frozen samples begins to increase with decreasing temperature, like for $Cu(tsPc)^{4-}$. It indicates that the spectral range 647−743 nm that so far has been assigned in the literature exclusively to the Q-band emission is also covered by the emission of other transient species that are stabilized at low temperatures. The results in Figures 3 and 4 indicate that the copper and zinc phthalocyanines have evidently different photochemical and photophysical channels of deactivation in the liquid phases. The difference may be related to the fact that zinc has the 3d subshell filled and filled deep enough to form rather pure molecular orbitals. In contrast, copper with the open 3d shells may result in a number of energetically close-lying electronic states[25] and charge transfer between the central metal and the phthalocyanine ligand or the electron transfer between the two adjacent phthalocyanine macrocycle rings may give contribution to these extra spectral features. The theoretical[25,30] and experimental results by resonant shift X-ray emission spectroscopy[43] show that there must be significant overlap between the phthalocyanine 2p character ligand states with the Cu^{2+} 3d states partially delocalized over the entire molecule. In contrast, zinc phthalocyanine exhibits a large gap between the HOMO and LUMO orbitals. The 3d-like b_{1g} orbital ($d_{x^2-y^2}$) lies much below the a_{1u} (HOMO) ligand orbital and represents the molecular orbital with much lower contribution from the metal 3d electrons than that for copper phthalocyanine[25] (see Scheme 1).

In contrast to normal fluorescence observed for $Zn(tsPc)^{4-}$ in the liquid phase, the frozen samples of $Cu(tsPc)^{4-}$ (and $Zn(tsPc)^{4-}$) show the opposite trend with decreasing temperature. It indicates that the emission in $Cu(tsPc)^{4-}$ at 682 nm, although it covers the same spectral range as the Q transition

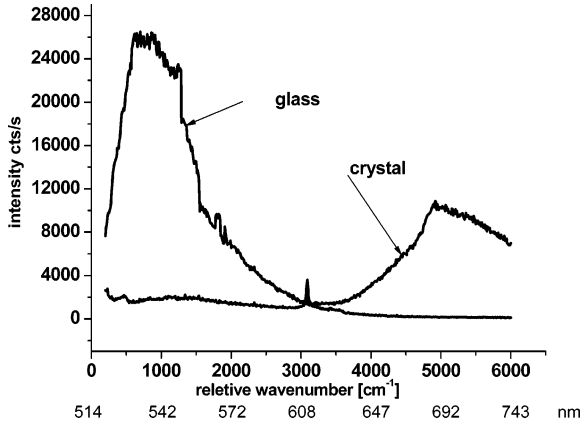

Figure 5. Raman spectrum of $Cu(tsPc)^{4-}$ in water for $c = 10^{-2}$ mol/dm^3 for the crystal and the glassy structures at 77 K.

fluorescence, should be assigned to the emission of transient species generated by light excitation. We have shown[1] that the energy of the visible light at 514 nm used in Raman spectrometer is sufficient to induce the photodissociation

$$[Cu(tsPc)^{4-}]_2 \xrightarrow{h\nu} Cu^{II}(tsPc^{\bullet})^{5-} + Cu^{II}(tsPc^{\bullet})^{3-} \qquad (1)$$

At room temperature the recombination processes are too fast to observe the emission of the transient species. At lower temperatures the molecular motions are slower, resulting in stabilization of the transient species that can be observed via their emission.

Striking behavior is revealed when we compare the photochemical properties for the glassy and the crystal phases. The results presented in Figures 3 and 4 represent the crystal phases generated in frozen samples. Figure 5 shows the results for the crystal and glassy phases of $Cu(tsPc)^{4-}$ in aqueous solution. The different phases have been generated by the various cooling rate. It is well-known that the fast cooling leads to glassy phases, whereas the slowly cooling generated the crystal phases. The generated phases have been monitored with the crystal phonon spectra in the range 15−400 cm^{-1} by Raman spectroscopy. Our results show evidently that the emission at 682 nm is observed only for the crystal phthalocyanine whereas is cannot be seen for the glassy phthalocyanine. In contrast, the emission at 520 nm that disappears at 77 K in the crystal phase is still observed in the glassy phase. The emission in the crystal phase and the lack of emission in the glassy phase clearly indicate that the emission at 682 nm represents the processes that are able to occur only in the ring-stacked crystal structures, but not in the frozen, disordered glassy structures (Chart 1).

The crystal polymorphs of $Cu(tsPc)^{4-}$ form ring-stacked columns[43,44] close enough in distance to overlap efficiently between the π-electronic clouds of the phthalocyanine macrocycle rings, and as a consequence, the photoinduced electron transfer between the adjacent rings occurs, leading to the photoinduced dissociation and generation of the radicals $Cu^{II}(tsPc^{\bullet})^{-5}$, $Cu^{II}(tsPc^{\bullet})^{-3}$ (eq 1). In our recent paper[1] we have assigned the emission at 682 nm to the transient species generated in the photoinduced dissociation due to the electron transfer between the adjacent copper phthalocyanine ligands (Scheme 2).

One can see from Figure 5 that in contrast to the emission at 682 nm the emission at 520 nm can be easily seen in the glassy phase of $Cu(tsPc)^{4-}$ in water at 77 K. Moreover, comparing Figures 3a and 5, one can see that the band at 520 nm that exists only for the liquid and undercooled aqueous solutions at 294−265 K and disappears at low temperatures for the crystal

CHART 1: (A) Ring-Stacked Crystal Structure; (B) Disordered Glassy Structure

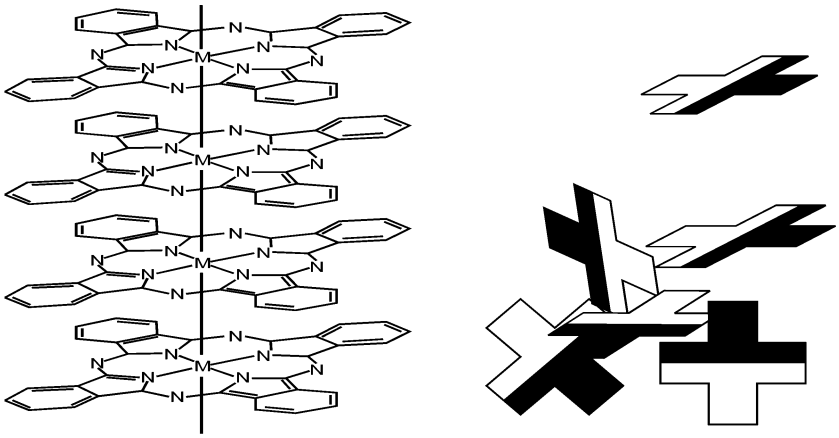

a) b)

SCHEME 2: Intermolecular Electron Transfer in the Crystal Phase of $Cu(tsPc)^{4-}$

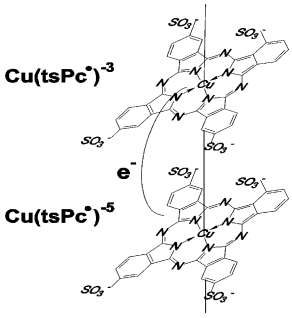

phase (250−77 K) (Figure 3a) still exists in the glassy phase at 77 K (Figure 5). It looks like photochemical properties of the liquid state have been preserved in the strongly amorphous glassy phase. It suggests that the emission at 520 nm has rather intramolecular origin in contrast to the emission at 682 nm that has evidently intermolecular origin.

The results in Figure 5 clearly indicate that the structure of $Cu(tsPc)^{4-}$ has a profound influence on the photochemical behavior. The crystal polymorphs of $Cu(tsPc)^{4-}$ that form the ring-stacked columns with the overlapping between the π-electronic clouds of the phthalocyanine macrocycles make possible the photoinduced electron transfer between the adjacent rings (eq 1). The emission at 682 nm in Figure 5 is related to this process and represents the transient radicals (or a radical) generated by the photodissociation (eq 1). In contrast to the crystal phases, the liquid solutions (Figure 3a) and amorphous glassy phases at 77 K (Figure 5) are only partially organized (Chart 1). As a consequence, the distances between the adjacent phthalocyanine rings are longer and the overlapping between the π-electrons is much less efficient, resulting in much less efficient photoinduced electron transfer. That is why we do not observe the 682 nm emission for the glassy phase at 77 K in Figure 5, although it is clearly seen at 77 K for the crystal phase (Figures 3a−c and Figure 5). However, the emission at 520 nm is clearly visible at 77 K for the glassy phase, which provides evidence that the emission at 520 nm represents the intramolecular mechanism and does not depend on the ordering and the structure of the frozen samples.

To elucidate further the nature of the transient species represented by the emission band at 682 nm and the origin of the emission at 520 nm in Figure 3a−c, we applied the femtosecond transient absorption pump−probe spectroscopy. We will show that combining the femtosecond spectroscopy and the low temperature Raman spectroscopy leads to a much clearer interpretation of photochemical and photophysical events in metal phthalocyanines than is possible from the stationary spectroscopic methods.

Figure 6 shows the transient absorption changes ΔA as a function of wavelength for a few delay times between the pump and probe pulses.

The negative ΔA signals at 600−635 and 670 nm correspond to the photobleaching of the $S_0(a_{1u}) \rightarrow S_1(2e_g)$ transition (Q-band) for the dimer and monomer, respectively. The positive

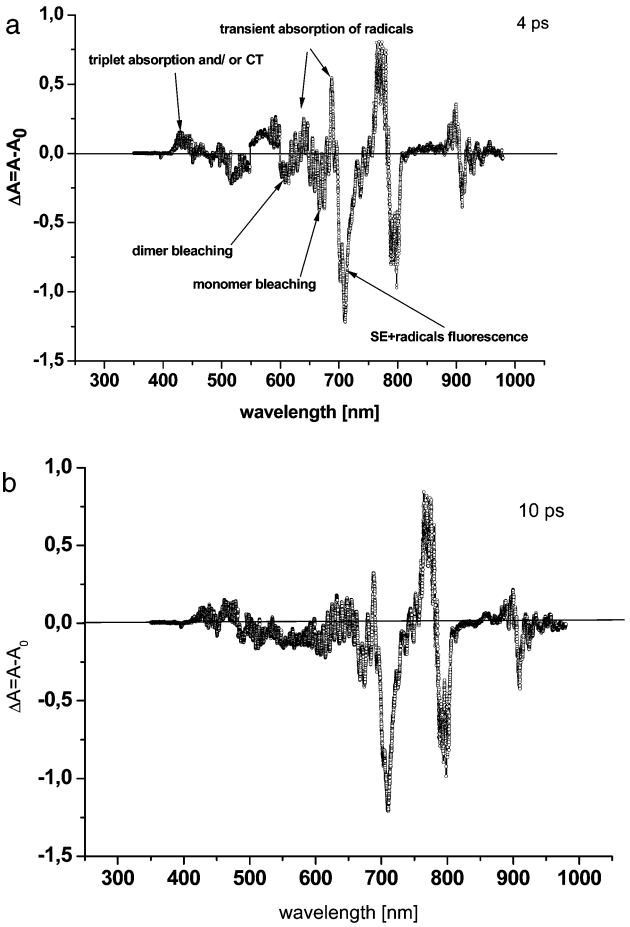

Figure 6. Transient absorption changes ΔA as a function of wavelength for a few delay times between the pump and probe pulses: (a) 4 ps; (b) 10 ps.

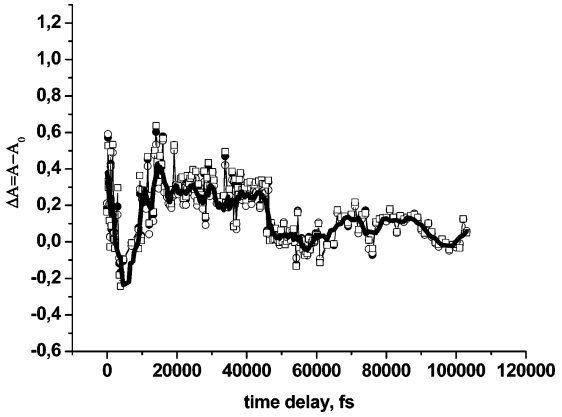

Figure 7. Transient signal of absorption change ΔA as a function of delay time at 611 nm (○), 618 nm (●) and 624 nm (□).

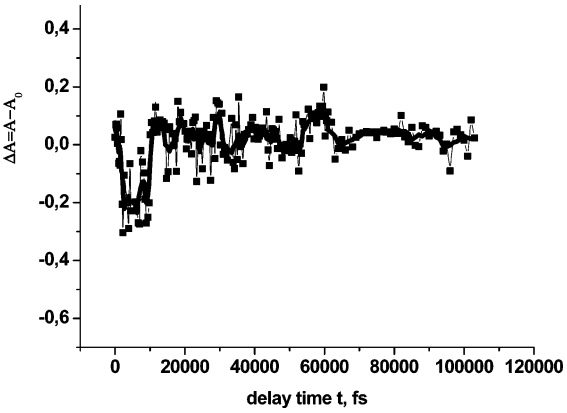

Figure 8. Transient signal of absorption change ΔA of $Cu(tsPc)^{4-}$ in water for $c = 6 \times 10^{-5}$ mol/dm^3 as a function of delay time at 398 nm.

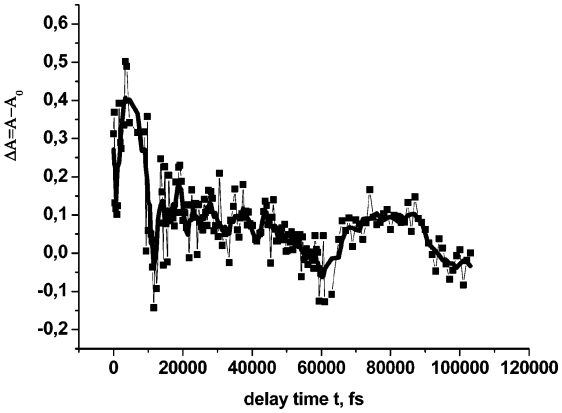

Figure 9. Transient signal of absorption change ΔA of $Cu(tsPc)^{4-}$ in water for $c = 6 \times 10^{-5}$ mol/dm^3 as a function of delay time at 949 nm.

ΔA signals at 645 and 688 nm correspond to the transient absorption ligand−ligand radicals generated in the process of photodissociation. The negative ΔA signal with minimum at 710 nm corresponds to the stimulated emission $S_1(2e_g) \rightarrow S_0(a_{1u})$ and transient radicals emission, which are observed immediately after excitation at 0 fs. The reason for these assignments will be discussed in detail below.

Figures 7−10 show the transient absorption changes ΔA as a function of delay time between the pump and probe pulses for several characteristic wavelengths at 618, 624, 398, 460, 949 nm, where $\Delta A = A - A_0$, A corresponds to the absorption of $Cu(tsPc)^{4-}$ in water solution when both the pump and the probe pulses are employed, A_0 corresponds to the absorption without the pump pulse.

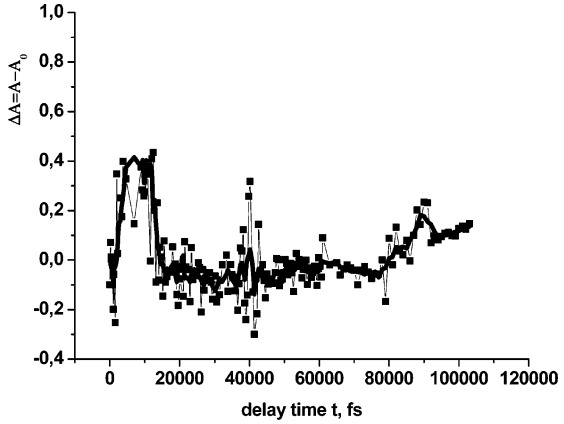

Figure 10. Transient signal of absorption change $\Delta A/A_0$ of $Cu(tsPc)^{4-}$ in water for $c = 6 \times 10^{-5}$ mol/dm^3 as a function of delay time at 460 nm.

In Figure 7 one can observe the positive ΔA signal at 611, 618 and 624 nm, immediately at zero delay that corresponds to the transient absorption, which indicates that the transient species are formed within the instrument response time. Then, at longer delay times the ΔA becomes negative, which indicates that the signal is dominated by bleach with a decay time of 6.7 ps. The transient absorption minimum is observed at around 5 ps and the signal is followed by a recovery with the rise time of 12.6 ps. The recovery goes beyond the zero at around 10 ps, which indicates that the transient absorption of a longer-lived species is still present. The transient absorption signal decreases with the decay time of 29.5 ps to zero.

To discuss the femtosecond dynamics features that can be rationalized from the transient signals of absorption ΔA as a function of delay between the pump and the probe pulses, we have to know the orbital levels that are excited with the pump pulse. The recent calculations of the electronic structure in metal phthalocyanines including copper and zinc phthalocyanines are very helpful in this discussion,[25] although the calculated transition energies for the Q and B bands are underestimated by 0.2−0.6 and 0.4−0.8 eV, respectively. Moreover, effects of peripherical substituents, especially the strongly electron-withdrawing groups from the Pc ring are able to change the ground state of metal phthalocyanine. Scheme 2 shows the molecular orbitals of the CuPc and ZnPc according to the calculations from ref 25 and the pump and probe wavelengths employed in our pump−probe femtosecond experiment.

We can see from Scheme 1 that the pump pulse at 398 nm can excite the $S_0(a_{1u}) \rightarrow S_n(b_{1u})$ transition (Q transition) and the $S_0(a_{2u}) \rightarrow S_1(2e_g)$ transition at the longer wavelength edge of the B band (maximum at 347 nm). Thus, probing with the pulses at 624 and 398 nm allows us to monitor the repopulation of the $S_0(a_{1u})$ and $S_0(a_{2u})$ states, respectively. Probing with the 460 nm and 949 nm makes possible monitoring the transient absorption $b_{1g}(d_{x^2-y^2}) \rightarrow S_n(b_{1u})$ and $b_{1g}(d_{x^2-y^2}) \rightarrow S_1(2e_g)$, respectively.

From the comparison between the results obtained from the femtosecond spectroscopy in Figures 6−10 and the electronic transitions presented in Scheme 1, the picture that is illustrated in Scheme 3 emerges.

The photochemical events are initiated by absorption of pump photons at 398 nm. The energy of the photon is in the resonance with the $S_0(a_{1u}) \rightarrow S_2(b_{1u})$ transition (Q transition to the second excited state) and with the longer wavelength wing of the S_0-

SCHEME 3: Primary Events in Terasulfonated Copper Phthalocyanine Initiated by Absorption of Pump Photons at 398 nm Employed in the Experiment

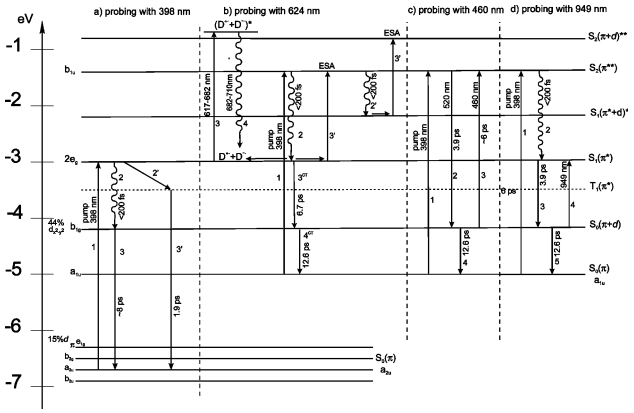

SCHEME 4: Deactivation of the $S_2(b_{1u})$ State for the $S_2(b_{1u}) \rightarrow S_0(a_{1u})$ Transition

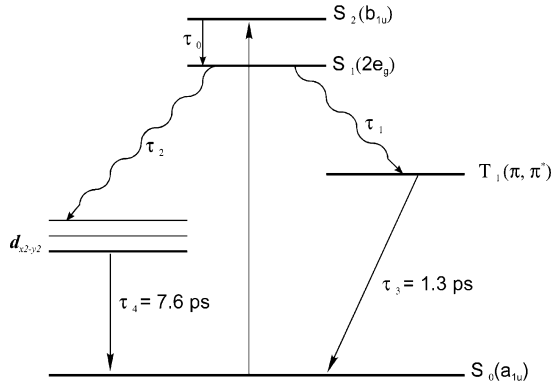

$(a_{2u}) \rightarrow S_1(2e_g)$ transition (B band). The absorption of a photon at 398 nm may result in the following events:

(1) $S_0(a_{2u}) \rightarrow S_1(2e_g)$ Transition. It represents the $S_0(a_{2u}) \rightarrow S_1(2e_g)$ transition of the electron from the ground ligand state $S_0(a_{2u})$ to the lowest lying (LUMO) excited electronic state $S_1(2e_g)$, which is delocalized over the entire phthalocyanine ligand of 2p character ($\pi \rightarrow p^*$). The excitation to the $S_1(2e_g)$ state leads to the depletion of the $S_0(a_{2u})$ state and the photobleaching corresponding to the negative transient absorption ΔA signal observed in Figure 8. The photobleaching signal recovers to zero after about 10 ps, which indicates that the excited molecules return to the ground state $S_0(a_{2u})$ within 10 ps. The photobleaching signal completely recovers to the initial zero level. The recovery has two components: slow one (~8 ps) and the fast one (1.9 ps). These lifetimes are in good agreement with those obtained by Rogers et al.[30] for cobalt (CoCrPc) and nickel (NiCrPc) phthalocyanines, for which such a fast repopulation of the ground state has been reported. Roger et al.[34] noticed that these times are shorter than those in hemes or other porphyrins. They have suggested that the repopulation in hemes and porphyrins is due to the intermolecular redistribution of excess energy to solvent or protein in heme. In contrast, the high density of vibrational states within the π-bonded network of phthalocyanine ligand may result in intramolecular path, which is an order of magnitude more rapid. They suggested that the repopulation from the $S_2(b_{1u})$ to the ground $S_0(a_{1u})$ state comes from two directions (Scheme 4): from the triplet $T_1{}^3$ ($\pi \rightarrow p^*$) state (faster component 1.3 ps) and the 3d states of the metal center (slower component 7.6 ps).

τ_0, τ_1, τ_2 constants are very fast and comparable with the instrumental response. The processes of repopulation to the S_0 state are fast because they represent the redistribution of excess vibrational energy between the vibrational levels of the high density of oscillators within the π-bonded network of the phthalocyanine ligand (τ_3) and from the metal-centered oscillators into the π-bonded oscillators of the ring (τ_4). We propose that similar mechanisms occur for the $S_0(a_{2u}) \rightarrow S_1(2e_g)$ transition excited at 398 nm (except the τ_0 path in Scheme 4) of the sulfonated copper phthalocyanine $Cu(tsPc)^{4-}$.

(2) $S_0(a_{1u}) \rightarrow S_2(b_{1u})$ Transition. Photoredox Dissociation Path. The excitation to the second excited $S_2(b_{1u})$ state leads to the depletion of the $S_0(a_{1u})$ state and the photobleaching corresponding to the negative transient absorption signal ΔA in Figure 7. However, in contrast to the results in Figure 8, at zero delay we observe a strong positive signal of ΔA that corresponds to the transient absorption. We have assigned it to the excited state absorption (ESA) for the transition $S_1(\pi^*) \rightarrow S_2(\pi^{**})$ or/and the charge transfer absorption due to the partial delocalization of the charge from the ligand to the central metal $S_1(\pi+d)^* \rightarrow S_2(\pi+d)^{**}$. Initially, the signal is dominated by the transient absorption; at longer times photobleach due to the depletion of the $S_0(a_{1u})$ state begins to dominate and results in the negative signal in Figure 7. The recovery goes beyond the zero at longer times, which indicates that there exists a long-living transient product that absorbs at around 624 nm. The lifetime of this product is 29.5 ps. We have assigned this transient product to the transient radical (reduced or oxidized form of the sulfonated copper phthalocyanine) generated in the photoredox dissociation[1]

$$[Cu^{II}(tsPc)^{4-}]_2 \xrightarrow{h\nu = 398\ nm} Cu^{II}(tsPc^{\bullet})^{5-} + Cu^{II}(tsPc^{\bullet})^{3-} \quad (2)$$

The photoredox dissociation (eq 2) leads to the electron transfer between the adjacent molecules resulting in formation of the ligand radical species. One of the radicals (or both radicals) has an emission at 682 nm that we observe by Raman spectroscopy (Figure 3a−c) and at 710 nm by the pump−probe femtosecond transient absorption (Figure 6). Indeeed, the positive signal at 710 nm in Figure 6 may partially belong to the stimulated emission SE from the $S_1(\pi^*)$ state, but it also corresponds quite well to the emission of the low temperature transient species observed by the Raman spectroscopy. The Raman intensity of the radical emission increases with decreasing temperature because the process of recombination becomes much slower at low temperatures and the transient species are stabilized at low temperatures. Moreover, at low temperatures the distance between the adjacent rings in the ring-stacked structures with overlapping between the π-electronic clouds becomes shorter and the intermolecular electron transfer channel becomes more efficient. At room temperature no emission is observed at 682 nm (Figure 3a−c) because the transient radicals live for a short period of time (estimated as 29.5ps from our pump−probe measurements).

(3) $S_0(a_{1u}) \rightarrow S_2(b_{1u})$ Transition. Charge Transfer Path. The photoredox dissociation is not the only process that occurs after the excitation with 398 nm. Another channel is presented in Scheme 3. This channel can be monitored with the probing pulses at 949 and 460 nm in the pump−probe transient absorption experiment presented in this paper. This channel represents fast deactivation occurring within the instrumental response time (<200 fs) to the $S_1(2e_g)$ state followed by the repopulation to the $S_0(\pi+d)$ with the time constant of 6.7 ps state and the repopulation to the ground state $S_0(a_{1u})$ with the time constant of 12.6 ps (Scheme 3b). When the molecule is in the $S_0(\pi+d)$ state, it can absorb photons via two possible

transitions: $S_0(\pi+d) \rightarrow S_1(2e_g)$ (at 949 nm, Scheme 3d)) and $S_0(\pi+d) \rightarrow S_2(b_{1u})$ (at 460 nm, Scheme 3c). The femtosecond results at 460 nm and 949 nm presented in Figures 9 and 10 provide excellent evidence in supporting these channels of deactivation. Indeed, for both 460 and 949 nm we observe positive signals that can be assigned to the transient absorption from the $S_0(\pi+d)$ state to the $S_2(b_{1u})$ and $S_1(2e_g)$, respectively. The $S_0(\pi+d)$ state is depopulated within about 10−15 ps according to the time constants calculated from the results in Figures 9 and 10, which corresponds quite well to the time constant of 12.5ps obtained for the 625 nm. Thus, the emission at 520 nm observed by Raman spectroscopy (Figure 3a,b) at 294−265 K for the liquid phase can be assigned to the emission $S_2(b_{1u}) \rightarrow S_0(\pi+d)$ from the charge transfer species (CT) (Scheme 3c). The charge transfer species can be produced as a result of the charge redistribution from the metal center to the ligand phthalocyanine ring or from the ligand phthalocyanine to the metal. It has been calculated[25] that for CuPc the one-electron oxidation occurs from the $S_0(a_{1u})$ state although the $S_0(\pi+d)$ state lies same 0.5 eV higher. Thus, the absorption at 949 and 460 nm (Figures 8 and 9) and the emission at 520 nm (Figure 3a,b) have been assigned to the ligand−metal charge transfer species. This CT mechanism assumes that the excitation initially deposited in the π-system of the ligand phthalocyanine is rapidly redistributed over the entire complex, including the $d_{x^2-y^2}$ state of the Cu^{2+} metal center. At lower temperatures, when the crystal phase is produced, the CT mechanism becomes much less efficient (the intensity at 520 nm disappears in Figures 3 and 5) due to the strong competition with the photodissociation channel (eq 2) that becomes much more efficient at lower temperatures (the intensity at 682 nm increases with decreasing temperature in Figures 3 and 5). The isobestic point at around 608 nm between these competitive processes can be clearly visible from Figure 3.

However, the photodissociation is effective only in the crystal phases. For the glassy phases the CT mechanism still operates because there is no competition with the channel 2 for the photodissociation. That is why we observe the emission due to CT species at 520 nm at 77 K in glasses whereas no emission at 682 nm of the photoinduced radicals can be seen (Figure 5).

In our recent paper[1] we suggested that the emission at 520 nm observed by Raman spectroscopy originates from the $T_n \rightarrow T_1$ transition. Similar suggestions have been given previously in refs 30 and 34 on the basis of the results obtained by the femtosecond pump−probe absorption spectroscopy. Rogers et al.[30] proposed a mechanism presented in Scheme 4 suggesting that the repopulation of the ground state $S_0(a_{1u})$ comes from the two directions: via the charge transfer CT states ($\tau_0 \rightarrow \tau_2 \rightarrow \tau_1$ path in Scheme 4) or via the triplet states of the ligand ($\tau_0 \rightarrow \tau_1 \rightarrow \tau_3$ path in Scheme 4). Tran-Thi et al.[34] have assigned the transient absorption at around 500 nm to the $T_1 \rightarrow T_n$ excited state absorption from the tri-doublet (^{2}T) and tri-quartet (^{4}T) states using the doublet-quartet splitting picture by Gouterman et al.[45]

However, the results presented in this paper seem to suggest that the ultrafast dynamics of the transient absorption at around 460 nm (and the emission at 520 nm) as well as the transient absorption at 949 nm is dominated by the charge transfer ligand−metal species rather than the triplet transition. It seems that the triplet transitions influence the longer scale dynamics. As we have noticed, the transient absorption signals (Figures 9 and 10) do not completely recover to the initial zero level far above 100 ps, suggesting that a small amount (≤10%) of a longer-lived component still exists. These longer-lived components may be related to the triplet transitions. This conclusion seems to support the suggestions by Rogers et al.[30] that the intersystem crossing $S_1(2e_g) \rightarrow {}^2T$ ($^2S_1$ and ^2T in Gouterman's picture) that occurs within the rise time of the ultrafast setup is followed by the decay ^2T state. The decay ^2T state undergoes branching: slow process leading to ^4T and fast process leading to another state (CT) that rapidly decays to the ground state $S_0(a_{1u})$ ($^2S_0$ in Gouterman's picture).

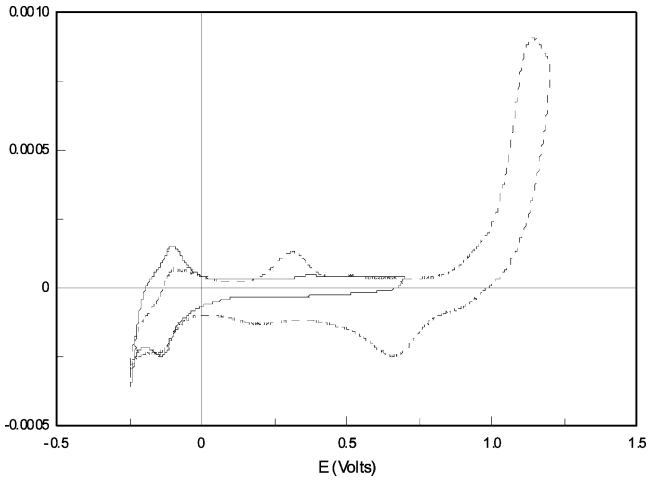

Figure 11. Voltammetric curves for $Cu(tsPc)^{4-}$ in water solution (c = 0.001 mol/dm^3) in 1 mol/dm^3 $HClO_4$, υ = 200 mV/s on gold electrode.

Some authors[24] have assigned the emission at 520 nm to the reduced form $Zn(tsPc)^{\bullet-}$ of the sulfonated zinc phthalocyanine. However, our Raman results in Figure 3a for $Cu(tsPc)^{4-}$ and in Figure 4 for $Zn(tsPc)^{4-}$ show that the emission at 520 nm decreases with decreasing temperature whereas the emission at 682 nm increases with decreasing temperature with the isosbestic point at around 608 nm. Thus, we can expect that it is rather the emission at 682 nm that should be assigned to the reduced (or oxidized) form of $Cu(tsPc)^{4-}$ than the emission at 520 nm that exhibits the features typical for the "normal" fluorescence.

Additional evidence related to the formation of CT species is provided by the electrochemical measurements.

Figure 11 presents voltammetric curves of complex of copper with sulfonated phthalocyanine ($Cu(tsPc)^{4-}$) in an aqueous solution of perchloric (VII) acid of concentration 1 mol/dm^3. The anodic and cathodic peaks occurring at potentials about −0.15 V correspond to redox reaction of the system Cu(II)−$(tsPc)^{4-}$/Cu(I)−$(tsPc)^{4-}$. The symmetry of these peaks and a small difference in the peaks' potentials (0.085 V) indicate the reversibility of the process. At potentials of about 0.3 V an additional peak appears on the curves. It is the peak coming from the reaction of oxidation of noncomplexed ions of copper. The additional peak appears only when the electrode becomes polarized with potentials over 1.1 V. At potential 1.13 V, the peak of the oxidation of the complex is visible. It may indicate that this stage of oxidation still leads to the decomposition of the particles of the complex and the release of the ions of copper.

Figure 12 presents voltammetric curves of solutions of zinc complexes with phthalocyanine ($Zn(tsPc)^{4-}$) in 1 mol/dm^3 $HClO_4$. The peaks of the redox system Zn(II)−$(tsPc)^{4-}$/Zn(0)−$(tsPc)^{4-}$ are visible on the curves at potentials about −0.07 V.

At potential 1.13 V the oxidation peak, similar to the peak at potential 1.13 V for copper phthalocyanine, appears. However, in case of zinc phthalocyanine, the decomposition of the complex is not observed.

In both cases of the examined complexes, the peaks on the voltammetric curves at potential 1.13 V are very similar to each

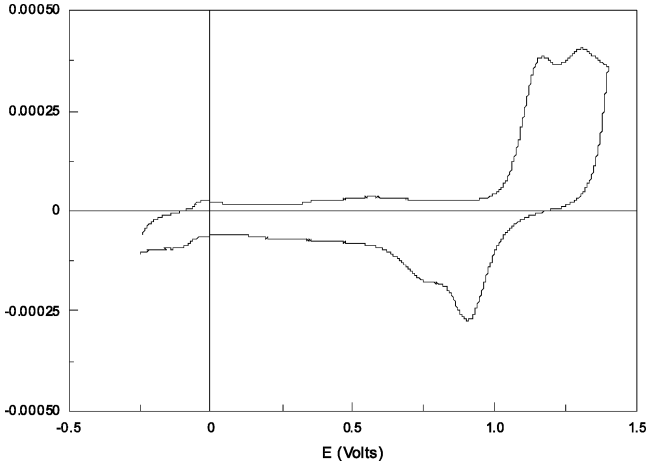

Figure 12. Voltammetric curves for $Zn(tsPc)^{4-}$ in water solution (c = 0.001 mol/dm^3) in 1 mol/dm^3 $HClO_4$, υ = 200 mV/s on gold electrode.

other. They are probably connected with the oxidation process of the ligand particles. In the solutions of the copper phthalocyanine the oxidation of the ligand particle, the process of inner electron transfer occurs, leading to the formation of charge transfer CT species that may result in the decomposition of the complex and the release of the ions of copper at higher potentials. In the case of the zinc complexes, either the inner electron transfer does not proceed or the process is possible but it does not cause the decomposition of the complex.

4. Conclusions

The systematic Raman and femtosecond pump−probe spectroscopy studies have been focused on a number of photochemical and photophysical properties of the sulfonated copper phthalocyanine. Some results for the sulfonated zinc phthalocyanine have been provided for comparison.

We have proposed the mechanisms of the primary events in the sulfonated copper phthalocyanine initiated by absorption of a photon from the violet range (398 nm). The energy of the excitation is in the resonance with the low energy wing of the Soret transition ($S_0(a_{2u}) \rightarrow S_1(2e_g)$) and with the maximum of the Q transition to the second lying excited state ($S_0(a_{1u}) \rightarrow S_2(b_{1u})$). The excitation corresponding to the Soret transition is deactivated rapidly within the instrumental response to the vibrationally excited manifold of the $d_{x^2-y^2}$ state and to the triplet T_1 state via the fast intersystem crossing from the $S_1(2e_g)$ state. Thus, the ground state $S_0(a_{2u})$ is repopulated from the two directions: from the $d_{x^2-y^2}$ state (slower component, ∼8 ps) and from the T_1 state (fast component, ∼1.9 ps) (Scheme 3a).

The excitation corresponding to the Q transition exhibits more complex pattern of behavior. After the pumping with 398 nm to the second excited state $S_2(b_{1u})$ two mechanisms are triggered:

(1) Photoredox Dissociation. The photoredox dissociation is accompanied by the electron transfer between the π-macrocycles of the adjacent phthalocyanine molecules in the ring-stacked structures, resulting in generation of the ligand-centered radicals ($D^{\bullet-} + D^{\bullet-}$) in Scheme 3b. The $S_2(b_{1u})$ state has rather too short a lifetime (<200 fs), to interact with the second macrocycle to the generate electron transfer between them. It seems that photodissociation (eq 1) occurs rather in the $S_1(2e_g)$ state (or in the $S_1(\pi+d)^*$ state) than in the $S_2(b_{1u})$ state. Otherwise, it would not be possible to generate the ligand-centered radicals with the 514 nm excitation as we observe in the Raman experiments in Figure 3. The ligand-centered transient radical (reduced, and/or oxidized) has a transient absorption in a spectral range similar to the range for the dimer of the copper phthalocyanine $[Cu(tsPc)^{4-}]_2$ (624 nm)[1] and the emission at 682 nm (Scheme 3b).

(2) CT Species Generation. The process of generation of ligand-centered radical occurs in the excited $S_1(\pi^*)$ or $S_1(\pi+d)^*$ states in competition with the formation of charge transfer species between the metal center and the phthalocyanine ligand. Thus, the excitation initially deposited in the phthalocyanine ligand macrocycle is rapidly partially distributed over the Cu^{2+} 3d states leading to the formation of the transient charge transfer (CT) species. The CT species relax within 3−6.7 ps to the ground state $S_0(\pi+d)$ (b_{1g}, 44% $d_{x^2-y^2}$), where they live for a relatively long time (∼12.6 ps). The CT species absorb at 460 nm ($S_0(\pi+d) \rightarrow S_2(b_{1u})$) and at 949 nm ($S_0(\pi+d) \rightarrow S_1(2e_g)^*$) (Scheme 3c,d), which can be clearly seen in our femtosecond pump−probe measurements as the transient absorption positive signals in Figures 9 and 10. This strongly indicates that the absorption at 460 nm observed by the femtosecond spectroscopy and the emission at 520 nm recorded by the Raman spectroscopy (Figure 3a) represent the same CT transient species formed between the metal center and the phthalocyanine ligand. However, the emission may partially origin from the additional channel of energy dissipation, namely $T_n \rightarrow T_1$ transition, as was suggested in the previous papers.[1,30,34] The triplet transient states seems to be important for longer times (>30 ps).

Moreover, combining the femtosecond absorption results with the low temperature emission spectra by Raman spectroscopy and comparing them with the theoretical results[25] for the orbital energy levels, we can exclude the other origins of the 520 nm emission in copper phthalocyanine suggested in the literature: (a) the reduced form of phthalocyanine, (b) $S_2(b_{1u}) \rightarrow S_0(a_{1u})$ emission, and (c) $S_1(2e_g) \rightarrow S_0(a_{2u})$ emission. Low temperature emission spectra by Raman spectroscopy have provided very strong evidence that the emission at 520 nm has intramolecular character (CT species or $T_n \rightarrow T_1$ emission) in contrast to the low temperature emission at 682 nm that has evidently intermolecular character and represents the ligand radical due to the electron transfer between the adjacent macrocycles in the ring-stacked structure.

Acknowledgment. We gratefully acknowledge the support of this work through the grant Nr3 T11E 04729 in 2005−2007. The support from the Dz. S/2006 is also acknowledged. We thank Dr. J. Suwalski, and J. Czerkawski for their assistance in low temperature Raman measurements and Dr. R. Kamiński for his assistance in degassing samples.

References and Notes

(1) Abramczyk, H.; Szymczyk, I.; Waliszewska G.; Lebioda A. *J. Phys. Chem. A* **2004**, *108*, 264.

(2) Abramczyk, H.; Szymczyk, I. In *Novel approaches to the Structure and Dynamics of Liquids: Experiments, Theories and Simulations*; Samios, J., Durov, V. A.. Eds.; Kluwer: New York, 2004; p 249.

(3) Szymczyk, I.; Abramczyk, H. *Pure Appl. Chem.* **2004**, *76*, 183.

(4) Abramczyk, H.; Szymczyk, I. *J. Mol. Liq.* **2004**, *110*, 51.

(5) Ferraudi, G. In *Phthalocyanines. Properties and Applications*; Lenzoff, C. C., Lever, A. B., Eds.; VCH Publishers: New York, 1989; p 321.

(6) Tokumaru, K. In *Phthalocyanines*; Shirai, H., Kobayashi, N., Eds.; IPC: Tokyo, 1997; p 170.

(7) Prasad, D. R.; Ferraudi, G. *Inorg. Chem.* **1982**, *21*, 2967.

(8) Muralidharan, S.; Ferraudi, G. *J. Phys. Chem.* **1983**, *87*, 4877.

(9) Ferraudi, G.; Muralidharan, S. *Inorg. Chem.* **1983**, *22*, 1369.

(10) Kaneko, Y.; Arai, T.; Sakarugi, H.; Tokumaru, K.; Pac, C. *J. Photochem. Photobiol. A: Chem.* **1996**, *97*, 155.

(11) Kaneko, Y.; Nishimura, Y.; Arai, T.; Sakuragi, H.; Tokumaru, K.; Matsunaga, D. *J. Photochem. Photobiol. A: Chem.* **1995**, *89*, 37.

(12) Kaneko, Y.; Nishimura, Y.; Takane, N.; Arai, T.; Sakuragi, H.; Tokumaru, K.; Kobayashi, N.; Matsunaga, D. *J. Photochem. Photobiol. A: Chem.* **1997**, *106*, 177.
(13) Howe, I.; Zhang, J. Z. *J. Phys. Chem. A* **1997**, *101*, 3207.
(14) Rückmann, I.; Zeug, A.; Herter, R.; Röder, B. *Photochem. Photobiol.* **1997**, *66*, 576.
(15) Chahraoui, D.; Valet, P.; Kossanyi, J. *Res. Chem. Intermed.* **1992**, *17*, 219.
(16) Kobayashi, N.; Ashida, T.; Osa, T. *Chem. Lett.* **1992**, 2031.
(17) Kobayashi, N.; Lever, A. B. P. *J. Am. Chem. Soc.* **1987**, *109*, 7433.
(18) Kobayashi, N.; Lam, H.; Nevin, W. A.; Leznoff, C. C.; Koyama, T.; Monden, A.; Shirai, H. *J. Am. Chem. Soc.* **1994**, *116*, 879.
(19) Kobayashi, N.; Togashi, M.; Osa, T.; Ishii, K.; Yamauchi, S.; Hino, H. *J. Am. Chem. Soc.* **1996**, *118*, 1073.
(20) Zhong, Q.; Wang, Z.; Liu, Y.; Zhu, Q.; Kong, F. *J. Chem. Phys.* **1996**, *105*, 5377.
(21) Strickler, S. J.; Berg, R. A. *J. Chem. Phys.* **1962**, *37*, 814.
(22) Gilbert, A.; Baggott, J. *Essentials of molecular Photochemistry*; Blackwell: Oxford, U.K., 1991; p 98.
(23) Rosenthal, I.; Krishna, C. M.; Riesz, P.; Ben-Hur, E. *Radiat. Res.* **1989**, *107*, 136.
(24) Tokumaru, K. *J. Porphyrins Phthalocyanines* **2001**, *5*, 77.
(25) Liao, M.-S.; Scheiner, S. *J. Chem. Phys.* **2001**, *114*, 9780.
(26) Liao, M.-S.; Watts, J. D.; Huang, M.-Ju; Gorun, S. M.; Kar, T.; Scheiner, S. *J. Chem. Theory Comput.* **2005**, *1*, 1201.
(27) Iglesias, R. S.; Segala, M.; Nicolan, M.; Gabezõn, B.; Stefanis, V.; Tores, T.; Livatto, P. R. *J. Mater. Chem.* **2002**, *12*, 1256.
(28) Carniato, S.; Luo, Y.; Agren, H. *Phys. Rev. B* **2001**, *63*, 85105.
(29) Liz, D.; Peng, Z.; Deng, L.; Shen, Y.; Zhou, Y. *Vibr. Spectrosc.* **2005**, *39*, 191.
(30) Nikolaitchik, A. V.; Korth, O.; Rodgers, M. A. J. *J. Phys Chem. A* **1999**, *103*, 7587.
(31) Howe, L.; Zhang, J. Z. *J. Phys. Chem. A* **1997**, *101*, 3207.
(32) Fourier, M.; Pépin, C.; Houde, D.; Ouellet, R. van Lier, J. E. *Photochem. Photobiol. Sci.* **2004**, *3*, 120.
(33) Howe, L.; Zhang, J. Z. *Photochem. Photobiol.* **1998**, *67*, 90.
(34) Tran-Thi, T. H.; Lipskier, J. F.; Houde, D.; Pepin, C.; Keszei, E.; Jay-Gerin, J. P. *J. Chem. Soc., Faraday. Trans.* **1992**, *88*, 2129.
(35) Nitzan, A.; Ratner, M. A. *Science* **2003**, *300*, 1384.
(36) Hersan, M. C.; Guighges, N. P.; Lyding, J. W. *Nanotechnology* **2000**, *11*, 70−76.
(37) Griffiths, J.; Schofield, J.; Wainwright, M.; Brown, S. B. *Dyes Pigments* **1997**, *33*, 56.
(38) Ioffe, I. S.; Dieviatova, N. I. *Zh. Obshch. Khim.* **1962**, *32*, 2111.
(39) Johari, G. P.; Hallbrucker, A.; Mayer, E. *J. Chem. Phys.* **1990**, *92*, 6743.
(40) Lever, A. B. P.; Pickens, S. R.; Minor, P. C.; Licoccia, S.; Rumaswany, B. S.; Magnell, K. *J. Am. Chem. Soc.* **1981**, *103*, 6850.
(41) Minor, P. C.; Gouterman, M.; Lever, A. B. P. *Inorg. Chem.* **1985**, *24*, 1894.
(42) Clack, D. W.; Yandle, J. R. *Inorg. Chem.* **1972**, *11*, 1738.
(43) Simon, J.; Bascoul, P. In *Phthalocyanines. Properties and Applications*; Leznoff, C. C., Lever, A. B., Eds.; VCH Publishers: New York, 1989; p 223.
(44) Dawnes, J. E.; McGuiness, C.; Glans, P. A.; Lernmonth, T.; Fu, T.; Sheridan, P.; Smith, K. E. *Chem. Phys. Lett.* **2004**, *390*, 203.
(45) Gouterman, M.; Mathies, R. A.; Smith, B. E.; Caughey, W. S. *J. Chem. Phys.* **1970**, *52*, 3795.